Ocean Dynamics Contribution to Seasonal Mixed Layer Heat Budget in the Tropical Atlantic

Jacques Servain[1,2] and Alban Lazar[3]

[1] *Institut de Recherche pour le Développement (IRD), UMR-182, Paris, France. Current affiliation at Fundação Cearense de Meteorologia e Recursos Hídricos (FUNCEME), Fortaleza, CE, Brazil*
[3] *Laboratoire d'Océanographie et du Climat : Expérimentations et Approches Numériques (LOCEAN), Université de Paris 6, Paris, France*
[2] *Corresponding author address: Jacques.Servain@gmail.com*

ABSTRACT

An Ocean General Circulation Model (ORCA-5) is used to investigate the relative magnitudes of the ocean dynamics components which contribute in the setting up of the seasonal mixed layer heat budget in the tropical Atlantic (25°N-25°S; 70°W-15°E). The analysis is carried out mainly inside boxes having a rather homogeneous dynamics. The ocean dynamics balance (from 10 to more than 100% of the atmospheric forcing) is strongly distinguished according to the different regions of the tropical basin. In general it opposes to the paramount warming or cooling effects by the atmospheric forcing during the both inversed hemispheric seasons. It continuously opposes with a range similar than that of the constantly positive atmospheric forcing in regions where seasonal upwellings occur (along the equator and off African coast). It also generally opposes with significant values (> 30%) to the atmospheric forcing in the ITCZ region. It adds the atmospheric forcing in few areas and during a limited time of the year. The vertical diffusion, the horizontal advection and the lateral diffusion are, by descending order, the most significant individual oceanic components which contribute to the seasonal mixed layer heat budget. The

prevalent vertical diffusion induces most of the time a cooling effect associated to Ekman pumping. The vertical diffusion is exceptionally positive (signal of inversion in the temperature profile) in the north-western region of the basin at beginning of boreal winter, *i.e.* when the surface waters cool quickly whereas subsurface waters remain hot after their strong summer heating. Such a positive contribution appears also with weaker values in the same region during the other semi-annual period, as well as along 10°S at west of 10°W, *i.e.* in the symmetrical region compared to the meteorological equator. The horizontal component of oceanic dynamics induces either a warming or a cooling effect when a strong surface current crosses a tighten SST gradient. Its warming effect, mainly associated to a transport of hot water coming from the equatorial latitudes, is positively prevalent during the warm season of each hemisphere from 15°N to 20°N at east of 40°W, from 5°S to 20°S at east of 10°W, and with broad of Brazil at south of 15°S. The lateral diffusion, always positive, occur with relatively weak values in limited regions as for instance along the equator and along the southern parts of the two continents. On the other hand it is exceptionally prevalent in the NW region (north of 5°N) which is subjected to the complex dynamics linked to a strong western edge ocean circulation.

Keywords: Tropical Atlantic Ocean, Seasonal mixed layer heat budget, Ocean dynamics

INTRODUCTION

In tropical latitudes, the heat flux balance coming from the atmosphere (radiative and turbulent fluxes) is of capital importance for the setting up of the seasonal mixed layer heat budget, and thus in the local variation of the sea surface temperature (SST). That drives, at first approximation, an unidimensional approach in the vertical going down direction for the dissipation of these heat fluxes, *i.e.* by making abstraction of all the advective phenomena (horizontal and vertical), those related to vertical and lateral turbulences, and those related to the energy transfers at the base of the mixing layer. The physical processes of this last series of variables, which are of oceanic nature, can however not be negligible, though, in a large part, they remain unfortunately still unknown, essentially because a not easily realizable observational access on a large space-time scale.

Here, our objective is to estimate, using a realistic numerical oceanic simulation, the relative importance of the oceanic variables which contribute to the setting up of the seasonal mixed layer heat budget (and thus of SST), to compare them *vs.* the terms of atmospheric nature (radiative and turbulent fluxes), and to compare their magnitudes between them. The numerical model is a climatic version of ORCA-05, one of the OGCM currently developed at LOCEAN. In this paper we examine more in details the tropical zones out of the equatorial band, the results on this equatorial band having already been the subject of another article (Peter et al., 2006).

The characteristics of the model are described in Section 2, as well as the methodology employed for our analysis, mainly based on monthly quantities called "trends", or variations from one month to another of the various studied variables. The main results are stated in Section 3, differentiating the variables by categories, and integrating those inside "boxes" having a similarly space homogeneity in the ocean dynamics. The discussion of the results is held according to a progression in the

complexity and the relative importance of the physical processes approached. A summarize of the principal results joints with the final discussion in the last section.

MODEL CONFIGURATION AND METHODOLOGY OF THE DIAGNOSTIC ANALYSES

The methodological basis of our analysis is the description, the discussion and the interpretation of the terms of tendency («trends») for the various analyzed variables. By the word «trend» one indicates the contribution, in degrees Celsius per time step, between two successive time steps of the model outputs (5 days), for each variable entering in the setting up of the seasonal variation of the SST (or more exactly the heat budget averaged inside the mixing layer). Positive (resp. negative) values of these trends thus express that each analyzed variable induced a warming (resp. cooling) of SST between two successive time steps.

Positive values of the SST trend (∂_tSST) occur when waters are heated from the thermal hollow of the cold season to the thermal maximum of the warm season. Negative values occur during the other period of the year when the waters are cooling. Both seasonal extremes of SST are thus concomitant with two passages by zero of ∂_tSST, and conversely, both extremes of ∂_tSST are concomitant with the most pronounced slopes in the annual evolution of SST. SST and ∂_tSST thus appear generally in squaring of phase. This may be different for the various components which contribute to the seasonal variation of SST. Indeed, it can prove that some of these components always keep the same sign all the year long, or they follow a more complex diagram as that of sinusoidal type.

ANALYSES OF THE MAIN RESULTS

Our objective is to measure the relative contribution of the oceanic terms entering in the seasonal variation of the heat budget of the mixing layer, and thus the seasonal variation

of the SST, *vs.* the contribution of the atmospheric terms. To facility the discussion we will use quantities which are summed or integrated over a monthly duration. The trends will be thus expressed in °C/Month.

The various quantities which will be discussed here (all will not be described in details) are as follows:

- NET LATENT HEAT FLUX=
- NET SENSIBLE HEAT FLUX=
- SHORTWAVE RADIATION ABSORPTION=
- NET LONGWAVE EMISSION=
- TOTAL_FORCING= the sum of the four terms above
- H_ADV = sum of zonal and meridional terms of the oceanic advection
- LATER = variation due to (mesoscale) horizontal turbulent diffusion
- HORIZ. OCEAN = H_ADV + LATER
- VERTICAL = VERTIC. OCEAN = sum of the vertical effects: adding vertical advection, vertical turbulence and entrainment at the base of the mixing layer
- TOTAL_OCEAN= sum of horizontal (H_ADV + LATER) and vertical (VERTICAL) oceanic terms
- DT_SST_ORCA= $d(SST\_ORCA)/dt = \partial_t SST_{ORCA}$ = variation of SST_ORCA (that must correspond to the sum of TOTAL_FORCING et TOTAL_OCEAN) (in °C/Month)
- SST_ORCA= Temperature of the mixing layer, simulated by ORCA (in °C)

In order to carry out a first space and time validation of the simulated outputs one will also use an observed SST climatology (Reynolds et al., 2002). There will be thus also the two variables:

- SST_REYNOLDS= observed SST climatology (in °C)
- DT_SST_REYNOLDS = $d(SST\_REYNOLDS)/dt = \partial_t SST_{Reynolds}$ = variation of SST_REYNOLDS (in °C/Month)

Finally, variables related to radiative fluxes (RAD) and turbulent fluxes (TUR) will be useful in the discussion:

- FLX_RAD_MLD
- FLX_TUR_MLD
- FLX_MLD = FLX_RAD_MLD + FLX_TUR_MLD
- FLX_RAD_70
- FLX_TUR_70
- FLX_70 = FLX_RAD_70 + FLX_TUR_70

These three first quantities are carried out from surface until the simulated mixing layer depth (MLD) which varies seasonally and locally. The three last quantities account for the same type of computation, but using a constant 70m depth, *i.e.* a coarse seasonal average of MLD on the whole basin. Comparisons of these quantities will allow a differentiated approach of the atmospheric forcing according to local and seasonal variations of MLD. Let us note that the sum of radiative fluxes (FLX_RAD_MLD) and turbulent fluxes (FLX_TUR_MLD) computed on MLD corresponds at TOTAL_FORCING previously defined.

Basin-Scale Analysis

Let us start the analysis with a synthetic seasonal description of the principal quantities stated above, namely: the local SST variation ∂_tSST (i), the balance of the atmospheric forcing (ii), the balance of the oceanic components (iii), that last variable being separated here in the sum of the horizontal (iv) and vertical (v) oceanic trends. To note, the yearly sum of all atmospheric and oceanic components must be exactly equal to the local SST yearly variation. These quantities, averaged during two complementary half-year periods, are shown on four panels of Figure 1 (October-to-March) and Figure 2 (April-to-September). Panels a are related to ∂_tSST (shaded) where we also reported the observed SST (contours) from Reynolds et al. (2002), averaged during the same 6-month periods. The period

October-to-March (Fig. 1a) is primarily associated to a cooling (resp. warming) of the heat content for the northern (resp. southern) hemisphere, while the reverse is the rule for April-to-September (Fig. 2a). For both half-year periods, ∂tSST varies regionally from a practically zero-value in a 3-5° latitudinal width just at north of the equator (*i.e.* the zone of the warmest SST and the mean position of Inter-Tropical Convergence Zone, ITCZ), to highest values of about +/-2.00°C/Month in the poleward latitudes of the study zone, as well as in the eastern basin subjected to important seasonal upwelling.

Panels b of Figs. 1 and 2 show the balance of the oceanic components (contours) superimposed to the balance of the atmospheric forcing (shaded). A decomposition of the oceanic balance according to horizontal and vertical processes appears (shaded) on panels c and d respectively. These figures clearly show the paramount influence of the atmospheric forcing in the setting up of ∂tSST. That is especially the case in the subtropics where seasonal SST warming (resp. cooling) of both hemispheres occur during positive (resp. negative) atmospheric forcing. The dynamics along the equatorial zone is very different. Here, the balance of the atmospheric forcing is strongly positive (> +1.50°C/Month) during the twice 6-month periods, indicating that the surface ocean receives much more heat from the atmosphere throughout the year than it refunds. Because ∂tSST (see a panels) changes of sign during the annual cycle along the equator, the necessary balance of SST variation in that region must be restored by a marked influence of the ocean dynamics which opposes to the atmospheric forcing (see contours on b panels, or shading on c and d panels). The continuously strong negative balance of the vertical oceanic processes (and in very first place the vertical diffusion) contributes for much (see d panels) to closing the local energy balance in this equatorial band throughout the year. The horizontal oceanic term (see c panels) also contributes to a relatively important share, but

differentiated in space (*e.g.* a rather heating at north of equator, and a rather cooling in the south), and differentiated in time (*e.g.* a westwards intensification of the cold equatorial tongue during the boreal spring-summer). More information of seasonal dynamics in this equatorial band is founded in Peter et al. (2006).

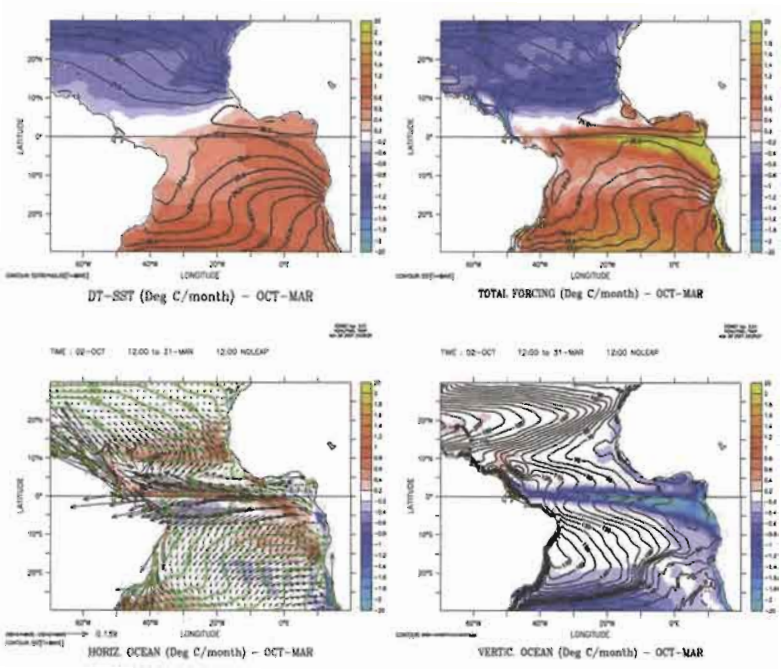

Figure 1 – *Quantities averaged during October-March. Top-left panel: Reynold's SST (black contours, °C) and SST monthly total variation (shaded, °C/Month); Top-right panel: Model SST (black contours, °C) and SST monthly variation due to total atmospheric forcing (shaded, °C/Month); Below-left panel: SST monthly variation due to horizontal oceanic processes (shaded, °C/Month), Model SST (green contours, °C) and surface currents (black arrows); Below-right panel: SST monthly variation due to vertical oceanic processes (shaded, °C/Month) and 20°C Depth (black contours, m). All the quantities come from ORCA Model, except Reynold's SST on topleft panel.*

Some points (which will be further discussed latter) can be identified when looking at more in details the lower panels of Figs. 1 and 2. Let us note for example the strong negative contribution of the oceanic vertical terms in the northern and southern tropics during the seasonal warming up of each hemisphere, *i.e.* where and when the Z20 is weak (see Z20 contours superimposed on d panels). This may be interpreted by vertical diffusive processes bringing up colder water from depths under a reduced mixing layer, itself strongly seasonally heated by atmosphere (see b panels). One notes also a strong importance of the oceanic terms (horizontal and vertical) along the continents. Finally, the charts of the horizontal oceanic terms (shaded on c panels), on which we superimposed the SST isotherms (green contours) as well as the surface currents (black arrows) provided by the model, clearly indicate how we can interpret positive or negative contributions by horizontal advection effect in the SST local change. That results in the combination between the pattern of the SST horizontal gradient and the pattern of the surface current. Thus, a SST warming by contribution of the horizontal advection is associated to a surface transport crossing a negative SST gradient (*i.e.* transport of warm water from higher isotherms towards lower isotherms), the reverse occurring for a transport of cold water through a positive SST gradient. More close to 90° the SST gradient and the surface current are crossing, more important the horizontal advection is efficient. Conversely, the influence of the horizontal advection in the seasonal variability of SST is extremely reduced when the surface current runs along the isotherms. Let us note however for memory, that this is the mean horizontal advection which is mainly responsible for the orientation of isotherms in the SST stationary state, what results in parallelism between surface current and isotherm directions.

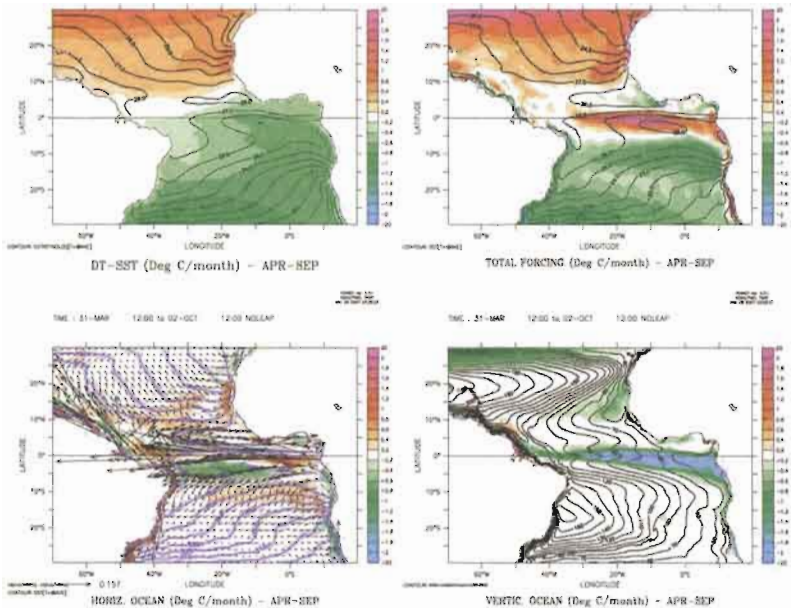

Figure 2 – *Same as Fig. 1 but for April-September.*

Regional Analysis

The commented study is limited here at north by 25°N, at south by 25°S, at east by the African continent, and at west by the American continent and 70°W. For a greater legibility of the results we carry out the analysis from isolated boxes. These boxes are regarded as representative of the principal regional characteristics associated to oceanic dynamics entering in the setting up of the heat budget of the mixing layer. For decision-making aid in the locations of these boxes, and after having tested among many criteria, we illustrate here the ratio (in %) between the yearly sum of the whole trends related to oceanic dynamics, and the absolute value of the yearly sum of the whole trends related to atmospheric forcing (Fig. 3). A weak percentage of the ratio (< |20| %) indicates a less influence

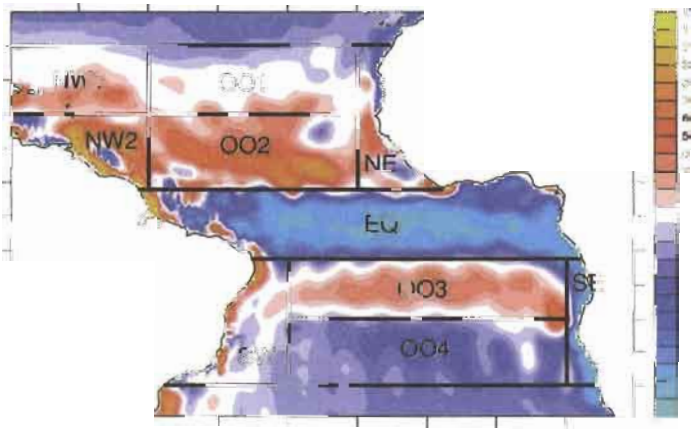
NW2
OO2
NE
Eq
SE
OO4

let us describe briefly the main geographical characteristics of each one of these ten boxes.

Boxes OO1, OO2, OO3 and OO4 are located in the open tropical basin. Boxes OO1 and OO2 (15°N-25°N/50°W-20°W and 4°N-15°N/50°W-20°W respectively) cover part of the North Equatorial Current (NEC), the North Equatorial Counter Current (NECC), the northeast trade winds, and are both mainly subjected to Ekman pumping. Box OO2 includes also the seasonal latitudinal transfer of ITCZ. Boxes OO3 and OO4 (6°S-15°S/30°W-10°E and 15°S-25°S/30°W-10°E respectively) are the symmetrical ones of the first two boxes for the southern hemisphere. These two boxes cover a good part of the South Equatorial Current (SEC), the southeast trade winds, and are also mainly under the influence of the Ekman pumping. Box EQ is located along the equator between 4°N and 6°S. It thus integrates the whole equatorial processes which are clarified in details according to a similar analysis in Peter and al., 2006.

Boxes NW1, NW2 and SW are localised in the west of the basin. Boxes NW1 (15°N-25°N/70°W-50°W) and NW2 (0°N-15°N/70°W-50°W), located at the north-west of the study zone, have rather different characteristics, the southern box being especially subject to western boundary dynamics off the American coast. We will see thereafter that Box NW1, at the entry of the Caribbean Sea, has some exceptional characteristics associated with inversion in the vertical profile of temperature. Box SW, located at broad of the Brazilian coast, is limited at open boundaries by 30°W, 6°S and 25°S. This box includes the termination of the westward South Equatorial Current (SEC) in its eastern region, and the Brazilian Current (BC) which is running southward along the Brazilian coast. BC is fed by a part of the SEC divergence flow, the other part of this flow moving northwards and giving rise to the North Brazilian Current (NBC) in the northern region of the box.

Two last boxes, symmetrically located on both sides of the equator along the African continent (from 4°N to 25°N at west

of 20°W for Box NE; from 6°S to 25°S at west of 10°E for Box SE) take into account the coastal seasonal upwellings, which are very efficient in these areas. The seasonal-and-regional variability of these phenomena being relatively complex we will supplement sometimes our matter by analyses at a more reduced space-time scale.

Seasonal evolutions of the atmospheric and oceanic trend variables entering into the balance of $\partial t/SST$, integrated in space for each one of the ten boxes previously defined, are described according to a sequential way (Figs. 4 to 13). The discussion begins (Fig. 4) with the equatorial box (EQ), what is the occasion to recall some results of Peter et al. (2006). The analyse description continues with the boxes where the oceanic processes remain relatively weak and few (the northern tropical ocean, as seen on Fig. 3), then runs on with the boxes where the oceanic processes are more important, and finishes with the boxes where these processes are definitely more complex (*e.g.* the upwelling regions). For each one of Figs. 4 to 13 we present two panels. The first panels (panels a) represent the seasonal evolution of SST (from ORCA-5), the monthly ∂_t/SST (both from ORCA-5 and from Reynolds), as well as the both atmospheric and oceanic monthly trend balances which are at the origin of $\partial_t SST$. The more efficient oceanic trends of each box (individually analyzed and/or summed by category) are seasonally detailed on the second panels (panels b), where we also reported (except for Box EQ) the radiative and turbulent fluxes vertically dissipated on either the really simulated MLD, or a constant 70m depth.

For all the time diagrams which are presented on Figs. 4 to 13, we chose to describe the seasonal evolution from April to March (and not from January to December as usually done). This makes it possible to discuss more easily the separate warming and cooling seasons for each studied region.

The Equatorial Band (Box EQ): An Intensive Contribution of Multiple Ocean Dynamics

Figure 4 relates to the equatorial Box EQ (4°N-6°S). SST (Fig. 4a) reaches its highest values (28.3°C) in March-April and its lowest values (25.2°C) in August, *i.e.* during the deep seasonal upwelling. Averaged over Box EQ, the model correctly reproduces the SST, with a negative error *vs.* the Reynolds's SST (not shown) lower than 0.5°C all along the year. In the same way, simulated and observed ∂_tSST are very close (Fig. 4a), except for two limited periods around June and October when the ORCA's cooling and warming are slightly too weak respectively. Here, the ocean continuously receives heat from the atmospheric forcing (see also Figs. 1b & 2b), with highest positive values varying from +0.75 to +1.40°C/Month between September and February, and weaker positive values during the remainder of the year. The atmospheric forcing is even close to zero value in May-June. The whole ocean contribution is continuously strongly negative throughout the year, with values ranging between -0.50 and -1.25°C/Month, thus practically of the same order of magnitude as those of atmospheric forcing. The analysis by individual term of the oceanic processes (Fig. 4b) shows that this is the vertical diffusion which contributes more to a permanent cooling effect of the mixing layer temperature, reaching -1.00°C/Month in May-June. The horizontal oceanic advection roughly follows the annual cycle of the atmospheric forcing, oscillating coarsely between slightly positive values (< +0.20°C/Month) between August and April, and more strongly negative values (-0.25°C/Month) in May-June, thus intensifying the cooling effect by vertical mixing. This pronounced negative ocean contribution occurs at the early setting up of the equatorial upwelling, when a strong westwards current crosses an intense east-west negative

gradient of the isotherms (*e.g.* see Fig. 2c). The lateral diffusion associated to tropical instability waves (TIW) is a third oceanic element responsible for the seasonal variation of SST (Foltz et al., 2003). Its effect, continuously positive, though weak (< +0.20°C/Month), is more sensitive in early boreal summer, at the moment of the optimal extension of the equatorial cold water tongue. It thwarts thus in partly the negative contribution by horizontal advection. For more details on the full seasonal dynamics of this equatorial area one can refer, for instance, to Peter et al. (2006) for a similar numerical study and Foltz et al. (2003) for an observed data analysis.

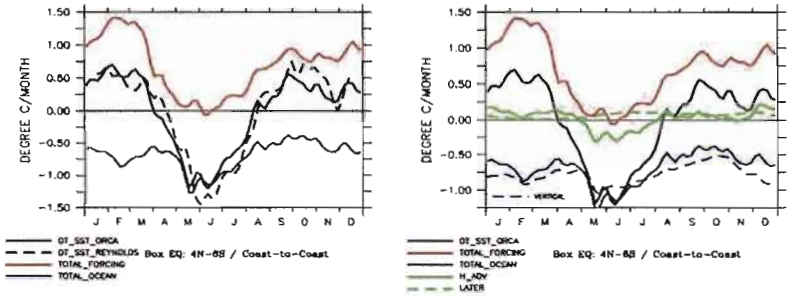

Figure 4 – *Seasonal evolutions (in °C/Month) of the atmospheric and oceanic trend variables entering into the balance of ∂t/SST, integrated in space for Box EQ (see Fig. 3). Left: Simulated SST evolution (continuous black), observed SST evolution (broken black), SST seasonal evolution due to total atmospheric forcing (red), due to total oceanic processes (blue). Right: Continuous red and blue curves (at left) are repeated; SST seasonal evolution due to oceanic horizontal advection (continuous green), due to oceanic lateral processes (broken green), due to oceanic vertical processes (broken blue).*

Open Ocean Regions Where the Vertical Diffusion is a Prevalent Oceanic Contribution (Boxes 001, 004 and NW1)

Figures 5 and 6 relate to Boxes 001 and 004, *i.e.* the two boxes in the open ocean the furthest away from the equator (Fig. 3). We discuss them simultaneously because they are of similar dynamics, though obviously with hemispheric opposition of phase. In both cases the model accuracy is particularly correct, the simulated SST being constantly slightly colder (< -0.2°C) as the Reynold's reference (not shown), and the simulated and observed ∂_tSST being very similar (Figs. 5a & 6a). The peak-to-peak amplitudes of the seasonal SST variations are also comparable (3.7°C in the case of OO1, 4.5°C in the case of OO4). Here, the local influence of the atmosphere is particularly dominant, with an obvious strong positive (resp. negative) role during the summer (resp. winter) season of each hemisphere.

The positive atmospheric balance contribution of ∂tSST for Box OO1 (Fig. 5a) is high and relatively constant between April and August (about +0.75°C/Month), with a very small decrease around July. This slight decrease is due to a light reduction in the radiative flux (not shown), itself related to a greater nebulosity associated with the most northern position of ITCZ at that time of the year. Atmospheric forcing and ∂tSST decrease together very quickly from the August high level to a deeply cooling in December (-1.25°C/Month), before to increase again until the April-to-August level. Box OO1, which includes the northern branch of the NEC, is a region with quasi permanent northwestward surface currents which are parallel with the isotherms (see Figs. 1c & 2c). These currents remain relatively weak throughout the year in the northern part of this box. In the southern part, they intensify slightly during the boreal summer, setting up a meridional velocity gradient which supports an increasing Ekman pumping. As illustrated

on Fig. 3, the balance of oceanic variable partially responsible for ∂_tSST in Box OO1 is extremely reduced *vs.* the atmospheric forcing. Always in opposition of phase with this last variable, it oscillates from values very slightly positive (< +0.10°C/Month) from November to March, to values slightly negative (< -0.20°C/Month) during the remainder of the year (Fig. 5a). The analysis by individual variables (Fig. 5b) indicates that the vertical diffusion, always negative, is mainly at the origin of the oceanic action in the setting up of the seasonal heat content variation of the surface mixing layer. Its highest negative action occurs during the warm season (April to October), *i.e.* when the surface heating by the atmosphere is the most intense, and the thermal profile stratification is the most important. The vertical mixing is almost equal to zero from November to March, what indicates that the positive low values of the oceanic balance contribution are due essentially to horizontal terms. The weak positive influence of the horizontal terms for this box (< +0.10°C/Month) reflects the fact that isotherms are practically always parallel with oceanic circulation (see Figs. 1c and 2c).

Differently to what occurs for Box OO1, the oceanic contribution for ∂_tSST is continuously negative (from -0.10 to -0.50°C/Month) for Box OO4 (Fig. 6). This cooling effect is mainly due to the vertical mixing with the deeper layers. That is especially the case in the southern part of the Box OO4 during the October-to-March period (see Figs. 1d & 6b), *i.e.* during the austral warm season, when the positive atmospheric forcing and the vertical oceanic stratification are at their highest levels. The oceanic contribution by horizontal advection (Fig. 6b) remains weak and negative (< -0.15°C/Month) all the year, with some intensification during the austral summer (see also Fig. 1c), when the SEC transports relatively cold surface waters coming from the south-east Atlantic.

Figure 7 is related to the Box NW1, an intermediate area between the open North tropical Atlantic basin and the entry of

the Gulf of Mexico. Here the surface currents are fairly linked to the North Atlantic cyclonic gyre. They run rather in the westward direction during the semi-annual period October-to-March (Fig. 1c), and rather in a northward direction during the rest of the year (Fig. 2c). As for the two preceding boxes, the simulated SST in Box NW1 is somewhat too cold compared to the Reynolds' observations (not shown), with a seasonal accuracy varying from a near zero value (in October for example) to more consequent values (-0.6°C in January-February). Simulated and observed curves of ∂_tSST are however very close throughout the year (Fig. 7a). With regard to the atmospheric forcing, there is a marked difference between Boxes OO1 and NW1: the positive plate which had been previously noted on Box OO1 from May to August does not exist for Box NW1. On the contrary, the positive thermal maximum is sharply marked during May (+1.50°C/ Month) for Box NW1. This is the consequence of a strong positive contribution of the radiative balance only (not sshown).

Similarly to Box OO1, the balance of the full oceanic action for Box NW1 passes by positive values (September-April) and negative values (May-August) never not exceeding I0.25I°C/ Month (Fig. 7). Similarly also with Box OO1, the vertical diffusion in Box NW1 is the preponderant factor for the (weak) oceanic contribution to the annual variation of SST (Fig. 7b). However, whereas this variable is continuously negative for Box OO1, it is sometimes negative or sometimes positive in the case of Box NW1. The negative values of this vertical diffusion are still associated with a cooling at the base of the mixing layer at the time of the maximum heating by the atmosphere (around May). The positive values of the vertical diffusion are associated with an inversion in the temperature profile within the first oceanic layers. That occurs mainly between October and January (see also Fig. 1c). A more detailed analysis (not shown here) confirms this unusual characteristic in the area of Box NW1.

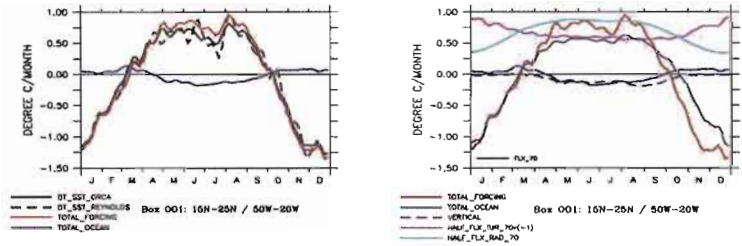

Figure 5 *– Seasonal evolutions (in °C/Month) of the atmospheric and oceanic trend variables entering into the balance of ∂t/SST, integrated in space for Box 001 (see Fig. 3). Left: Simulated SST evolution (continuous black), observed SST evolution (broken black), SST seasonal evolution due to total atmospheric forcing (red), due to total oceanic processes (blue). Right: Continuous red and blue curves (at left) are repeated; SST seasonal evolution due to oceanic vertical processes (broken blue). Black, purple and cyan curves are not discussed here.*

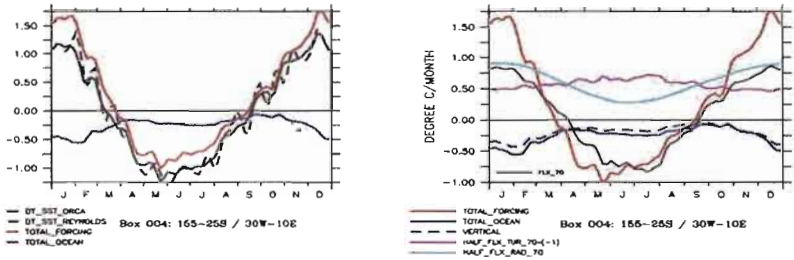

Figure 6 *– Same as Fig. 5 for Box 004.*

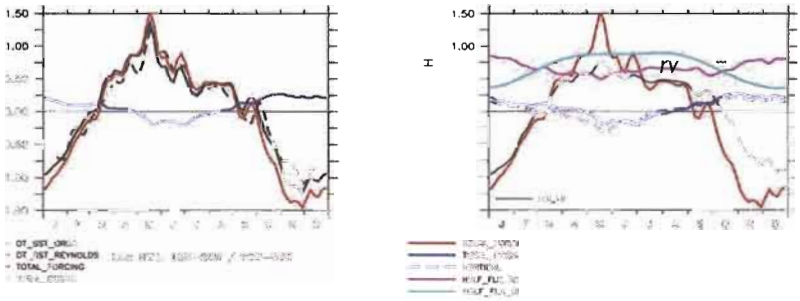

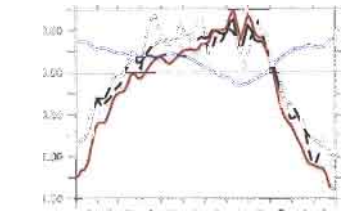

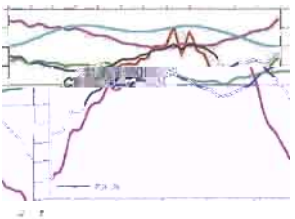

of -1.00°C in June-July). The balance of the oceanic terms is positive (or close to zero) most of the time, the only period with very weak negative values (< -0.10°C/Month) occurring in January-February. Two relative positive extremes are noted, a first one in April-May (+0.30°C/Month), a second one with half-value in November (+0.15°C/Month). Let us note a new characteristic, not yet observed in the discussion of the preceding boxes, namely that the balance of the oceanic terms results here from the addition of a continuously positive horizontal advection (with values not exceeding +0.30°C/Month, this one found in April), and continuously negative vertical terms (with values lower than -0.30°C/Month, that one found in February, *i.e.* at the moment of the maximum warming by the atmosphere). The continuously positive horizontal advection reflects an uninterrupted southward transport of warm waters from the equator in the region of Box OO3, quite visible on Figures 1c and 2c. A monthly more detailed study (not shown here) indicates that this oceanic warm transport is particularly strong at the time of changing of years. The most raised values, but of opposed signs, of the horizontal advection and the vertical turbulence appear during the warm season of the southern hemisphere (from November to April), whereas their lowest values meet during the opposite season (from May to October). Thus, for this Box OO3, the strong positive values of the atmospheric forcing during the southern warm season are reinforced, though moderately, by a positive contribution by advection coming from the equator, but are attenuated by a cooling of about the same amplitude mainly due to vertical turbulence. During the cold season (namely from June to September), these oceanic terms have a very small influence on the total balance of the variation of ∂tSST.

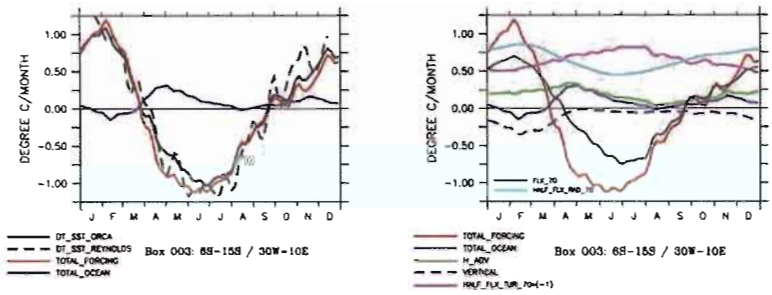

Figure 9 *– Same as Fig. 5 for Box OO3, except, SST seasonal evolution due to oceanic horizontal advection (green) is also plotted.*

Coastal Regions with a Complex Oceanic Contribution (Boxes SW, NW2, NE and SE)

It now remains to discuss the four boxes with a continental frontier, whether along America (Boxes SW and NW2), or along Africa (Boxes NE and SE). Because the dynamical oceanic processes along the continental shelves are generally very complex, and are often limited to a narrow littoral band, it is not easy to apprehend sufficiently homogeneous structures with the box dimensions thus defined. We will however endeavour to be the most complete possible in the analysis, in particular when the need is useful, by discussing physical processes developing in sub-boxes.

Let us begin the discussion with Box SW (Fig. 10). This box is the western continuation of Boxes OO3 and OO4 discussed previously. It corresponds to the prolongation and divergence of the SEC, with mainly here its southern branch, the BC, which runs southwards skirting the Brazilian coast. Integrated over Box SW, the seasonal variations of SST, ∂tSST and atmospheric forcing (Fig. 10a) are similar with those of Boxes OO2 and OO3. The representativeness of the model is however somewhat degraded in the case of Box SW, the simulated SST being systematically too cold *vs.* Reynolds' SST of a quantity ranging between 0.2 and 0.5°C (not shown).

The balance of the oceanic terms oscillates around zero (one time in October, another time in March) with a peak-to-peak amplitude of approximately 0.75°C/Month. It tends to counter the heating by atmospheric forcing effect during the warmest months of the year (November at March), and tends on the contrary to counter its cooling from April to August. During a short period of the year around September-October, just after the coldest SST peak occurring in August, the two processes add to heat the ocean.

The negative oceanic balance during the two first months of the year (Fig. 10b) is mainly due to the arithmetical addition of the horizontal advection (< -0.15°C/Month) and the sum of the vertical variables (< -0.50°C/Month). In December the horizontal effects being almost null, the vertical component induces alone (< -0.50°C/Month) the oceanic cooling action. The horizontal advection is weakly positive (< +0.25°C/Month) from April to October. This warm contribution by advection corresponds to the arrival of the southern branch of the SEC divergence, after having been heated during its westwards circuit near the equator. This southern branch forms the BC moving southwards along the Brazilian coast. The contribution by cold water advection at the very first beginning of year is more difficult to explain. Because the southern limit of Box SW (25°S) this cold water advection cannot have like origin the cold current of Maldives, running up northwards along the American continent between the north of Argentina and the south of Brazil. This cold current of Maldives is indeed practically never observed in the north of 30°S.

To finish with this box, let us note that the vertical oceanic effect, combined with the loss of heat by horizontal advection, involve a loss for the ocean of approximately -0.75°C/Month at the very beginning of year (January-February). This loss is however partly compensated by positive values (~ +0.25°C/Month) of mesoscale turbulence, particularly important for this area between December and March (Fig. 10b).

The two Boxes NE (Fig. 11) and SE (Fig. 12) illustrate seasonal upwelling regions boarding the African coast. Like the majority of other OGCMs, ORCA does not simulate sufficiently deep the seasonal cooling in these zones, though the phase of the seasonal SST variation is correctly represented.

Box NE (see Fig. 3) skirts the African coast from Mauritania (25°N) to Liberia (5°N). It integrates the seasonal upwelling (boreal winter) off Senegal, as well as the Guinea Dome (centred on 7°N-15°W) which is also a zone of water resurgence from June to September (Yamagata and Lizuka, 1995). In order to take into account these regional characteristics we proceeded (not shown here) to a cluster analysis between northern and southern parts of this box. This enables us to refine the discussion on some difficulties for dynamic interpretation. The northern part (25°N-15°N) of Box NE corresponds to a zone of permanent (Mauritania) and seasonal (Senegal) upwelling. Here, the SST annual variation is of sinusoidal type with a large amplitude, of which a thermal minimum occurring in February-March (~ 20.0°C according to Reynolds, called hereafter "atR") at the heart of upwelling, and a thermal maximum occurring in August-September (~ 25.0°C atR) which is directly connected to the largest heating of the boreal summer. The southern part (15°N-5°N) of Box NE is a zone with a strong latitudinal variability including the Guinea Dome area. Here, the SST variation is semi-annual (Yamagata and Lizuka, 1995) with two minima of different values, one in March (~ 26.0°C atR) and the other in August (~ 27.0°C atR), and two maxima of similar values, one in May-June (~ 28.0°C atR), and the other in November (28.5°C atR). This semi-annual variation, typical of this Guinea Dome area, is the consequence of an intense cooling which develops between June and September (thus between the two thermal maxima) thanks to a local divergence of the heat transport (Yamagata and Lizuka, 1995). Such a divergence is generated by a strong wind stress curl, itself associated to the

seasonal meridional migration of the North-East trade winds. The two thermal maxima seem to be associated with intrusions of coastal Kelvin waves coming from the equatorial area (Yamagata and Lizuka, 1995).

Integrated over the total surface of Box NE, the seasonal variation of the SST is of sinusoidal type (Fig. 11a). It presents a minimum (24.0°C atR, 25.5°C according to ORCA, called hereafter "atO") in March, and thus mainly relates the seasonal upwelling in the northern part of the box, as well as the first cooling (in March) of the southern part. The highest SST (27.0°C atR, 27.5°C atO) which occurs in October is the combination between the thermal maximum of the northern part (in September) and the second thermal maximum of the southern part (in November).

As debated just above, the SST ORCA simulation integrated into Box NE is somewhat further away from the Reynolds' SST reference. The error remains positive throughout the year, with values equal or higher than +0.5°C, and even reaches +1.5°C in February-March. The distinction between northern and southern sub-areas of this box informed us that the error comes to a large extent from the southern zone. Indeed, the error is practically constant (ranging between +0.5 and +1.0°C) for the northern zone, whereas it exceeds +1.7°C in March-April for the southern zone. On the other hand it is relatively weak for this southern part (between +0.2 and +0.5°C) the remainder of the year. But once again, if we focus the analysis on the ∂_tSST yearly variability, and making abstraction of the three months M-A-M, simulation and observation are quite similar (Fig. 11a). That enables us to remain confident in the representativeness of the trends of Box NE which are now discussed.

One notes for the Box NE a relatively good similitude, out of the M-A-M period, between the seasonal variability of atmospheric forcing and the seasonal variability of ∂_tSST (Fig. 11a). For both variables, a sharp cooling period occurs between

November and February (with a negative extreme of about -1.25°C/Month at the change of the year), and a period of heating the remainder of the time. During the warming phase there is moreover the same type of "setback" in June-July. This is the consequence of the seasonal passage of ITCZ athwart the box, and (Fig. 11b). This setback insulates two positive extremes for ∂_tSST and for its atmospheric forcing component. For ∂_tSST for instance, these positive extremes (~ +0.50°C/Month) appear around May and around August respectively.

Let us see now how the oceanic trends evolve for this region. The horizontal advection is slightly positive (< +0.25°C/Month) when it is calculated on the whole Box NE (Fig. 11b). The more detailed analysis by north and south sub-regions states however some discrepancies. This term remains positive (~ +0.25°C/Month) all the year for the northern part and from June to November for the southern part, but it becomes negative (~ -0.25°C/Month) between March and May for the southern part. A heating by advection is thus carried out on the whole Box NE during the second part of the year. During the first part of the year, the model indicates that the horizontal advection brings heat in the southern part (the nearest to the equator), and brings colder waters in the northern part. This last phenomenon must relate to the horizontal extension of the upwelling during the boreal winter in this region. An attentive monthly examination of the horizontal advection contribution to ∂_tSST (not shown here) makes it possible to note a northward displacement thru the time of positive values passing from 5-15°N between January and April, to 15-20°N between July and September.

Contrary to the horizontal advection component, the vertical diffusion integrated inside Box NE is always negative (with a maximum reaching -0.50°C/Month in April). This variable moves practically in phase with the full oceanic budget (Fig. 11b), the amplitude difference being obviously

+0.7°C) throughout the year for the southern zone. The errors of north and south sub-areas being both positive during the southern winter, and being opposed with the same order of magnitude the remainder of the year, it is thus coherent to find that the simulated SST for the whole Box SE seems too warm between June and October, and correct the remainder of the year. If one refers now, no longer with SST but with ∂_tSST (Fig. 12a), one notes that for the whole Box SE the model approaches rather well the observation, the error being really significant (± 0.50°C/Month) only between April and June (not enough cooling), and between September and November (not enough warming). The finer study using the north and south sub-areas previously defined indicates that only the northern zone of the Box SE is responsible for these errors of trends. For the southern zone, indeed, the seasonal variation of the SST provided by the model is into a relative good agreement throughout the year with the observation.

After checking a relative truth ground with the simulated ∂_tSST for Box SE, let us look at the most significant characteristics of the components responsible for this SST variation. Though both practically in phase, ∂_tSST and the atmospheric forcing have very different ranges (Fig. 12a). The atmospheric component is (almost) continuously positive, with values reaching +3.00°C/Month (the highest positive value in all this study) in December-January, and values close to zero from May to August. In other words, the surface ocean, for this specific area along the African coast, receives continuously more heat from the atmosphere that it refunds any. The seasonal variation of ∂_tSST (~ 3.00°C/Month peak-to-peak; here also the strongest value recorded in this study) passes from negative values (from April to August) to positive values (from August to April), and is always lower (in the arithmetic way) than the atmospheric forcing variation. This difference varies between 1.50 and 2.50°C/Month from November to June. It is more reduced (~

1.00°C/Month) the remainder of the year. That thus implies a very strong contribution of the ocean in the setting up of the seasonal variation of SST for this Box SE. The balance of the oceanic contribution is always negative throughout the year, which implies that it always opposes to the continuously positive atmospheric forcing. Extreme values (-2.25°C/Month) of this cooling effect by oceanic processes take place in December, while weaker, though again relatively strong negative values (-0.75 to -1.00°C/Month), take place from June to October.

Which are the most significant terms of oceanic components for this Box SE (Fig. 12b)? The sum of the vertical components, always negative, approaches very well the full balance of the oceanic components, either for phase or amplitude (from -0.50 to -1.50°C/Month). A more detailed analysis (not shown here) indicates that the vertical turbulence and the vertical advection enter each one with equal values for increasing the deep cooling of the mixing layer during the cold season (June-to-October), and also for reducing the heating during the warm season (November-to-March). The horizontal advection component is also always negative throughout the year. It is particularly important between December and June, with extremes values (~ -1.00°C/Month) around May. That corresponds to a cold water transport associated to the northwards Benguela Current running along the South Africa and Namibia coasts.

Note, like special characteristic of Box SE, that the lateral turbulence (Fig. 12b) is the only oceanic term of positive sign, though very weak (< +0.10°C/Month), throughout the year.

Now let us defer our attention in the northern hemisphere, and examine the case of Box NW2 located along and with broad of the American continent (Fig. 13). This box corresponds to the westward extension of Box OO2. Here also, ORCA does not represent very well the SST (not shown here). The simulated SST is systematically colder (~ -0.7°C) than the observed SST. However, if one refers to the seasonal variability of simulated

and observed ∂_tSST (Fig. 13a) one realizes, once again, that the simulation is very close to reality.

Contrary to the other cases studied until now, the signals of the trends are far to be sinusoidal for Box NW2. If ∂tSST reveals a very marked cooling during the boreal winter (from October to February), the period of heating during the remainder of the year is strongly attenuated during a few weeks around June. What is in charge for such setback? This is obviously not an oceanic effect because the budget of the oceanic terms is in continual opposition of phase with ∂tSST (Fig. 13a). This is the atmospheric forcing which causes this brutal reduction in the warming of SST.

The budget of the oceanic components (Fig. 13a) also moves on according to an original annual variation. It is positive practically during ten months; only the period August-September is slightly negative (< -0.25°C/Month). The positive period is complex with two extremes, one in December-January (+0.70°C/Month), and the other, weaker, in June (+0.30°C/Month), *i.e.* exactly during the setback discussed previously with the atmospheric forcing and ∂tSST.

The phase of the horizontal advection (Fig. 13b) is similar with that of the full oceanic budget, although the duration of the negative values is definitely larger for the horizontal advection (from May to November) than for the oceanic balance (August-September). The positive contribution of the horizontal advection during the boreal winter and beginning of the spring is easily comprehensible: heat is advected from the hot equatorial zones by water northward transport via the NBC. The significantly negative values (-0.25°C/Month) of this variable during August-September seem more delicate to interpret. They can be however explained by the fact that, at that time of the year, waters coming from the equatorial Atlantic, though with relatively high temperatures, remain colder of one or two degrees Celsius (see Fig. 2a) compared to the waters locally heated by the

very strong radiative net budget. Another originality for this Box NW2: The lateral turbulence is here of noticed importance, in particular by significantly positive values (~ +0.25°C/Month) throughout the year.

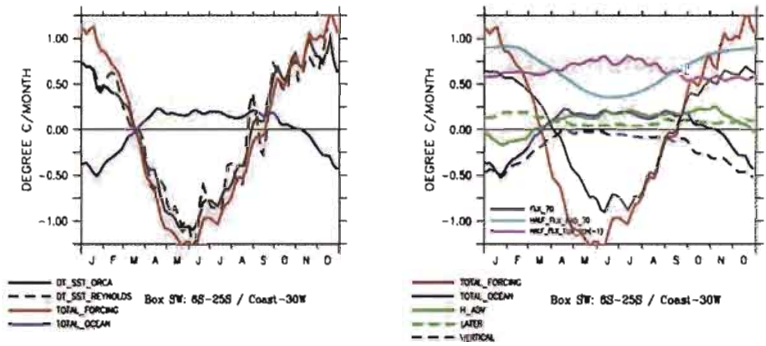

Figure 10 *– Same as Fig. 5 for Box SW, except, SST seasonal evolutions due to oceanic horizontal advection (green) and due to oceanic lateral processes (broken green) are also plotted.*

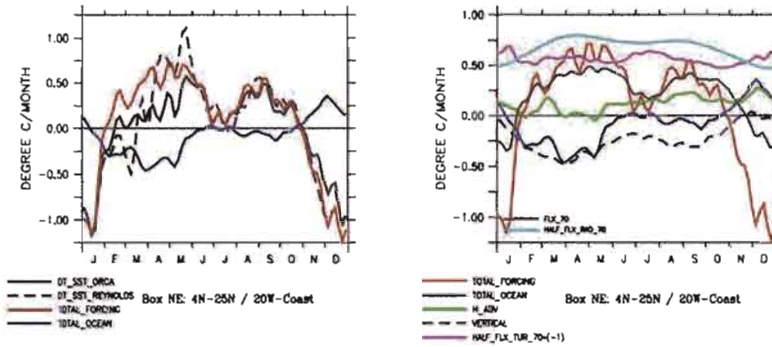

Figure 11 *– Same as Fig. 5 for Box NE.*

Although the sum of the horizontal components is responsible to a large extent of the oceanic total budget in this Box NW2, the vertical components contribute also with a positive share during the boreal winter. This vertical contribution, exceptionally positive, is to be brought closer to what we had already noted for Box NW1 located immediately at north (see Fig. 7b). A finer analysis (not shown here) indicates that it is mainly the term of vertical turbulence which is, here also, the principal factor for these positive values from December to February. That must be related to a striking inversion in the temperature profile which appears temporarily during the cold season in this area (see also Fig. 1c).

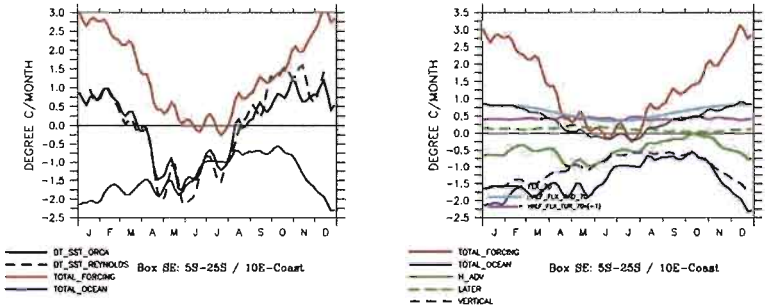

Figure 12 – *Same as Fig. 10 for Box SE.*

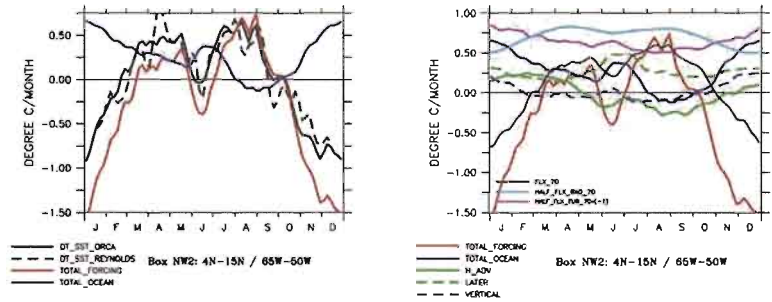

Figure 13 – *Same as Fig. 10 for Box NW2.*

SUMMARIZE AND FINAL DISCUSSION

Our objective was to improve the knowledge of atmospheric and oceanic components which contribute in the setting up of the seasonal mixed layer heat budget (*i.e.* roughly the SST) for the whole tropical Atlantic. In addition to a certain number of results which confirm former works on a broad scale, our regional approach made it possible to differentiate more in details numerous aspects of this dynamics. Let us summarize the main results according to the following items.

- The influence of the atmospheric forcing in the seasonal variation of SST is obviously essential inside the whole tropical basin, even in the regions where the oceanic dynamics contribution is also important. Because this paramount influence of the atmosphere, warming (resp. cooling) of heat budget generally follows pretty well the warming (resp. cooling) seasons for each hemisphere.
- In general, the effect of the budget of the oceanic dynamics opposes to the warming or the cooling effects of the net atmospheric forcing.
- The importance of the oceanic dynamics (from 10 to more than 100 % of the atmospheric forcing influence) is largely differenced according to various regions of the basin.
- In the open northern tropical basin along 20°N (Boxes NW1 and OO1), and in the open southern basin along 10°S (Box OO3), the seasonal variation of SST is largely dominated by fluctuation between warm and cold seasons imposed by the see-saw of the atmospheric forcing. Here, the limited, and generally opposite, oceanic contribution (less than 30 % of atmospheric forcing contribution) may result from the addition of very weak individual components (ex. Box OO1), or from somewhat conflict between relative higher values of these components (ex. Box OO3).
- Conversely, the oceanic dynamics is very important (with a range similar to that of atmospheric forcing) along the equator (Box EQ) and along the southern African coast (Box SE), *i.e.* where strong seasonal upwellings occur.

positive in Boxes OO2, OO3 and NE (warm water transport from equatorial zone). It is always strongly negative in Box SE and always weakly negative in Box OO4 (cold water transport from South Africa region). It is either forcefully positive or negative according to the season in other regions associated to intense current variability (Boxes EQ, NW2, SW). It is weak in

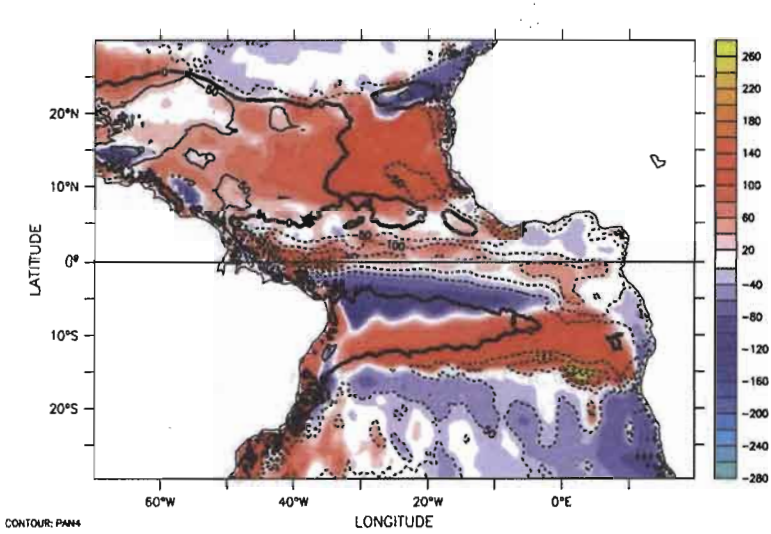

Figure 14 – *Ratio (%) of the budget of the horizontal oceanic contribution vs. the absolute value of the budget of the total oceanic contribution (shaded); Ratio (%) of budget of the vertical oceanic contribution vs. the absolute value of the budget of the total oceanic contribution (contours). These ratios are averaged in October-to-March for northern hemisphere, and in April-to-September for southern hemisphere.*

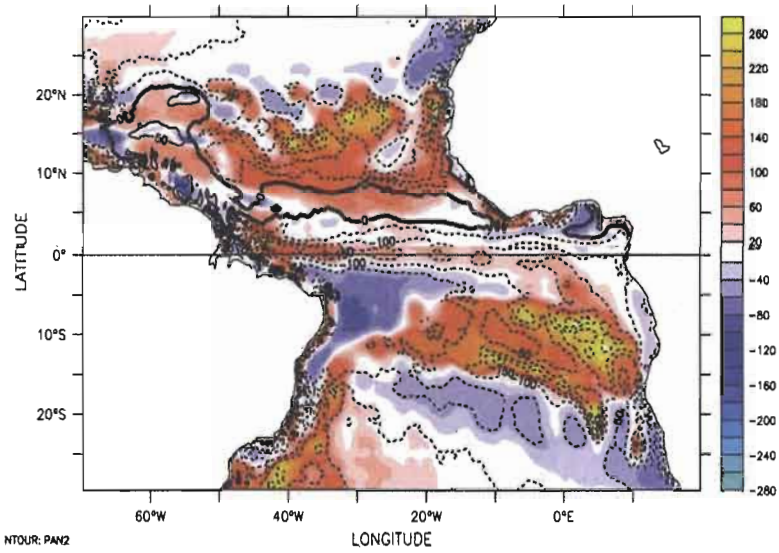

Figure 15 – *Same as Fig. 14, except the semi-annual periods are inversed.*

regions where the current is almost always parallel to the isotherms (Boxes NW1 and OO1).

- Oceanic significant effect by lateral diffusion, always positive, is limited to specific areas where the surface dynamics is complex (Boxes EQ, SW, SE, NW2). It is generally weak, except for Box NW2 where it is even of range superior with the two other oceanic variables (horizontal advection and vertical diffusion). That explains because many powerful mesoscale ocean dynamics coexist in this region (western boarding circulation, meanders development, counter-current formation, etc.).

After discussing the contribution of the various components of the ocean dynamics *vs.* atmospheric forcing in the setting up of the seasonal mixed layer heat budget, let us finish this discussion by comments of Figures 14 and 15 which illustrate the relative importance of horizontal *vs.* vertical ocean dynamics. We plotted on each one of these figures two ratios. A first one (shaded) is the ratio of the budget of the horizontal oceanic contribution *vs.* the absolute value of the budget of the total oceanic contribution. The second ratio (contours) is the budget of the vertical oceanic contribution *vs.* the absolute value of the budget of the total oceanic contribution. These ratios are averaged according to the same semi-annual periods as previously illustrated, *i.e.* April-to-September and October-to-March. These semi-annual periods are however differently combined so that Figure 14 relates the cooling period for both hemispheres, and Figure 15 relates the warming period also for both hemispheres. More information in the regional analysis of the oceanic dynamics is thus available, and that allows reinforcing and specifying some points of discussion as follow.

The patterns illustrated on Figs. 14 and 15 confirm relatively well the delimitation of the boxes which was made previously, with however a somewhat restriction for the region about the Box SW, where we encountered already some difficulties in the interpretation of oceanic variables when they are integrated in this full box (see discussion of Fig. 10). Here (shaded on Figs. 14 & 15) the ratio using the horizontal component is not locally homogenous, with bands either positive or negative, along or off the continent.

The patterns of Figs. 14 and 15 are relatively similar for both semi-annual periods, what is not really surprising because we already noted such a raw similarity on Figs. 1c,d and 2c,d where the horizontal and vertical components were independently plotted. Using the ratio now defined for Figs. 14 and 15, we note that the horizontal ocean dynamics is positively prevalent

during the warm season of each hemisphere (Fig. 15) for three regions: (i) from 15°N to 20°N at east of 40°W, (ii) from 5°S to 20°S at east of 10°W, and with broad of Brazil at south of 15°S. These patterns confirm also the very large distribution of negative contribution from the vertical oceanic component, with prevalent values during all the year along the equator and along the southern West Africa coast, and during the spring-summer period in the poleward regions. From another hand, these patterns show also, in an exemplary way, the prevalent positive contribution of the vertical oceanic component to the SST variation which occurs in the north-western basin during the boreal winter. Such a positive contribution appears also, though with limited values, in the same north-western region during the other semi-annual period, and along 10°S at west of 10°W, i.e. in the symmetrical region compared to the meteorological equator.

That study is being completed according to two angles: Firstly, an interannual analysis in order to differentiate the oceanic from the atmospheric causes for SST regional anomaly; Secondly, a local analysis focusing over the comparison between model outputs and available observed data (ex. the PIRATA data set), at least for some of the oceanic variables being able to be evaluated from direct measurements (advection, heat content, ...).

ACKNOWLEDGEMENTS

This work is part of the CNPq-IRD Project "Climate of the Tropical Atlantic and Impacts on the Northeast" (CATIN), N° CNPq Process 492690/2004-9.

REFERENCES

Filipe, V. L. L., 1997: The Angola Dome as observed in 1996. *ICES Council Meeting Papers, ICES, Copenhagen, Denmark,* 1997/EE14, 14 pp.

Foltz, G. R., S. A. Grodsky, and J. A. Carton, 2003: Seasonal mixed layer heat budget of the tropical Atlantic Ocean. *J. Ge-*

ophys. Res., 108(C5), 3146 , doi:10.1029/2002JC001584.

Grodsky, S. A., J. Carton, C. Provost, J. Servain, João A. Lorenzzetti, and M. J. McPhaden, 2005: Tropical instability waves at 0°N, 23°W in the Atlantic: A case study using Pilot Research Moored Array in the Tropical Atlantic (PIRATA) mooring data. *J. Geophys. Res.*, 110(C08010), doi:10.1029/2005/JC002941.

McClain, C. R., and J. Firestone: An investigation of Ekman upwelling in the North Atlantic. *J. Geophys. Res.*, 98(C7), 12,327-12,340.

Peter, A.-C., M. Le Hénaff, Y. du Penhoat, C. E. Menkes, F. Marin, J. Vialard, G. Caniaux, and A. Lazar, 2006: A model study of the seasonal mixed layer heat budget in the equatorial Atlantic. *J. Geophys. Res.*, 111(C06014), doi:10.1029/2005JC003157.

Reynolds, R. W., N. A. Rayner, T. M. Smith, D. C. Stokes, and W. Wang, 2002: An improved in situ and satellite SST analysis for climate. *J. Climate*, 15, 1609-1625.

Seidler, G., N. Zangenberg, R. Onken, and A. Morlière, 1992: Seasonal changes in the tropical Atlantic circulation: Observation and simulation of the Guinea Dome. *J. Geophys. Res.*, 97(C1), 703-715.

Signorini, S. R., R. G. Murtugudde, C. R. McLain, J. R. Christian, J. Picaut, and A. J. Busalacchi, 1999: Biological and physical signatures in the tropical and subtropical Atlantic. *J. Geophys. Res.*, 104(C8), 18,367-18,382.

Wang, J., and J. Carton, 2002: Seasonal heat budgets of the North Pacific and North Atlantic Oceans. *J. Phys. Oceanogr.*, Vol. 32, 3474-3489.

Xie, S.-P., and J. Carton, 2004: Tropical Atlantic variability: Patterns, mechanisms, and impacts. *Earth's Climate: The Ocean-Atmosphere Interaction Geophysical Monograph Series 147, Copyright 2004 by the American Geophysical Union*, 10.1029/147GM07, 121-142.

Yamagata, T., and S. Lizuka, 1995: Simulation of the tropical thermal domes in the Atlantic: A seasonal cycle. *J. Phys. Oceanogr.*, Vol. 25, 2129-2140.